https://doi.org/10.5194/egusphere-2022-716
Preprint. Discussion started: 8 August 2022

Revisiting the global mean ocean mass budget over 2005-2020

Anne Barnoud[1], Julia Pfeffer[1], Anny Cazenave[1,2], and Michaël Ablain[1]

[1]Magellium, 31520 Ramonville-Saint-Agne, France
[2]LEGOS, Toulouse, France

Correspondence: Anne Barnoud (anne.barnoud@magellium.fr)

Abstract. We investigate the continuity and stability of GRACE and GRACE Follow-On satellite gravimetric missions by assessing the ocean mass budget at global scale over 2005-2020, focusing on the last years of the record (2015-2020) when GRACE and GRACE Follow-On faced instrumental problems. For that purpose, we compare the global mean ocean mass estimates from GRACE and GRACE Follow-On to the sum of its contributions from Greenland, Antarctica, land glaciers and terrestrial water storage estimated with independent observations. A significant residual trend of -1.60 $\pm$ 0.36 mm/yr over 2015-2018 is observed. We also compare the gravimetry-based global mean ocean mass with the altimetry-based global mean sea level corrected for the thermosteric contribution. We estimate and correct for the drift of the wet tropospheric correction of the Jason-3 altimetry mission computed from the on-board radiometer. It accounts for about 40 % of the budget residual trend beyond 2015. After correction, the remaining residual trend amounts to -0.90 $\pm$ 0.78 mm/yr over 2015-2018 and -0.96 $\pm$ 0.48 mm/yr over 2015-2020. GRACE and GRACE Follow-On data might be responsible for part of the observed non-closure of the ocean mass budgets since 2015. However, we show that significant interannual variability is not well accounted for by the data used for the other components of the budget, including the thermosteric sea level and the terrestrial water storage. Besides, missing contributions from the evolution of the deep ocean or the atmospheric water vapour may also contribute.

1 Introduction

The increase in ocean mass due to land ice melting is responsible for about two thirds of the global mean sea level rise, which has major impacts for the populations living in coastal areas (e.g. IPCC, 2019; Horwath et al., 2022). Since 2002, the Gravity Recovery and Climate Experiment (GRACE; Tapley et al., 2019) and GRACE Follow-On (GRACE-FO; Landerer et al., 2020) satellite gravimetric missions allow monitoring the ocean mass variations from space as the gravity field is directly sensitive to the redistribution of water masses on land and in the oceans. These data are used to assess and understand the effects of climate change and climate variability on the Earth system, such as variations of freshwater storage (e.g. Vishwakarma et al., 2021), ice sheet melting (e.g. Velicogna et al., 2020; Shepherd et al., 2021), interannual variability of water mass transport (Pfeffer et al., 2022), variations of Earth's energy imbalance (Hakuba et al., 2021; Marti et al., 2022). Ensuring the stability of GRACE and GRACE-FO data is therefore very important for climate and hydrological applications. Both missions have encountered some instrumental problems due to battery and accelerometer failures (Bandikova et al., 2019). Moreover, the one-year gap between the GRACE and GRACE-FO missions has led to missing data between mid-2017 (end of GRACE life) and mid-2018 (launch of GRACE-FO data). Despite these issues, no bias between the two subsequent missions was reported by comparing GRACE

https://doi.org/10.5194/egusphere-2022-716
Preprint. Discussion started: 8 August 2022

and GRACE-FO data to independent estimates for specific components such as ice sheet mass loss (Velicogna et al., 2020) or terrestrial water storage variations (Landerer et al., 2020).

However, Chen et al. (2020) reported a non-closure of the global mean sea level budget as of 2016 by comparing the global mean ocean mass (GMOM) variations based on GRACE and GRACE-FO data to the altimetry-based global mean sea level (GMSL) variations corrected for the Argo-based global mean steric sea level variations. While 40 % of the non-closure was identified as the result of errors in salinity measurements of the Argo float (Barnoud et al., 2021), part of the non-closure remains unexplained and is potentially due to other components of the sea level budget, including the GRACE and GRACE-FO-based ocean mass. Here, we investigate whether the GRACE and GRACE-FO mass component may be responsible for the remaining non-closure of the GMSL budget observed over the most recent years (Barnoud et al., 2021). We focus on the recent years (beyond 2015) noting that the sea level and ocean mass budgets were successfully shown to be closed within uncertainties until 2016 (Horwath et al., 2022). Using state-of-the-art datasets, we assess the global mean ocean mass budget from January 2005. We compare the GRACE and GRACE-FO-based GMOM with the sum of individual mass contributions from independent data sources available until December 2018. These mass components include ice-mass losses from the ice sheets, ice caps and glaciers, and terrestrial water storage changes. We also compare the GMOM with the altimetry-based GMSL corrected for thermosteric effects until December 2020.

2 Method

2.1 Global mean ocean mass budget approach

The ocean mass budget consists in assessing the ocean mass change from independent observations. The global mean ocean mass change $\Delta GMOM$ can be broken down into its contributions as follows:

$$\Delta GMOM = \Delta GIS + \Delta AIS + \Delta GIC + \Delta TWS + \epsilon \quad (1)$$

Where ΔGIS, ΔAIS, ΔGIC and ΔTWS refer to Greenland and Antarctica ice sheets mass loss, glaciers and ice caps melting and terrestrial water storage changes. ϵ accounts for other potentially negligible contributions (e.g. atmospheric water vapour content and permafrost thawing) and data errors.

GMOM variations can also be estimated from GMSL changes corrected for the global mean steric sea level change due to temperature and salinity variations. At global scale, the mean halosteric sea level change due to salinity variations is negligible (Gregory and Lowe, 2000; Llovel et al., 2019), so that the global mean steric sea level change is nearly fully accounted for by the global mean thermosteric sea level changes $\Delta GMTSL$. Therefore, the $\Delta GMOM$ can be written as:

$$\Delta GMOM = \Delta GMSL - \Delta GMTSL + \epsilon' \quad (2)$$

where ϵ' accounts for potentially negligible remaining contributions, including the nearly null global mean halosteric sea level, and errors (e.g. due to the evolution of the deep ocean not sampled by the Argo float).

https://doi.org/10.5194/egusphere-2022-716
Preprint. Discussion started: 8 August 2022

2.2 Data processing

To assess the ocean mass budget, we rely on time series from observations and models. To ensure the consistency between the various datasets, we apply the same processing to each of them. For gridded ocean datasets, a restrictive mask is applied so that all data cover the same spatial extent. This mask excludes polar oceans (above 66° North and below 66° South), marginal seas and a buffer zone of 200 km from the coastlines to minimise leakage effects from land mass variations estimated by GRACE and GRACE-FO data (Dobslaw et al., 2020). The mask extent is shown in Figure SI1 of the supplementary information (SI). The global averages are weighted according to the surface of sea water within each grid cell. For each time series, annual and semi-annual signals are removed by least-square fitting, a three-months low-pass Lanczos filter is applied and the temporal average is removed. Some components of the budget are assessed from several available estimates. In such cases, the ensemble mean is computed as the average of the considered time series at each time step.

Uncertainties are assumed to be Gaussian and are provided as standard uncertainties, corresponding to the 68 % confidence level. When ensemble means are used to assess a component of the budget, the associated standard uncertainty σ is computed by combining the standard deviation σ_{ens} of the datasets included in the ensemble and the standard uncertainties $\sigma_{1\leq i\leq N}$ of the N individual time series when this information is provided, assumed independent:

$$\sigma = \sqrt{\sigma_{ens}^2 + \sum_{i=1}^{N} \sigma_i^3} \tag{3}$$

This approach is used for the contribution of Greenland and Antarctica ice sheets melting and for the thermosteric sea level component. When assessing the budgets, the uncertainties associated with the sum of the components and with the residuals are obtained by summing the variances of the individual components involved.

All linear trends given in this article are computed by an ordinary least-squares regression. The associated uncertainties are estimated using an extended ordinary least-squares method that takes into account the data uncertainties.

3 Data

3.1 GRACE/GRACE Follow-On data

We use six GRACE and GRACE-FO solutions from different processing centres, including three mass concentration (mascon) solutions and three spherical harmonics solutions. The mascon solutions are the Release 6 from the Jet Propulsion Laboratory (JPL; Watkins et al., 2015), the Center for Space Research (CSR; Save et al., 2016; Save, 2020) and the Goddard Space Flight Center (GSFC; Loomis et al., 2019). Over the oceans, the mascon solutions are provided as ocean bottom pressure data, with the ocean and atmospheric loading effects included. To obtain the ocean mass change, the spatial mean of the GAD product (Dobslaw et al., 2017), accounting for the static atmospheric surface pressure, is removed from the mascon data (Chen et al., 2019). We also use spherical harmonics solutions up to degree 60, including the Release 6 of the JPL, CSR (Bettadpur, 2018) and German Research Center for Geosciences (GZF; Bettadpur, 2018; Dahle et al., 2018, 2019). These data are provided as

https://doi.org/10.5194/egusphere-2022-716
Preprint. Discussion started: 8 August 2022

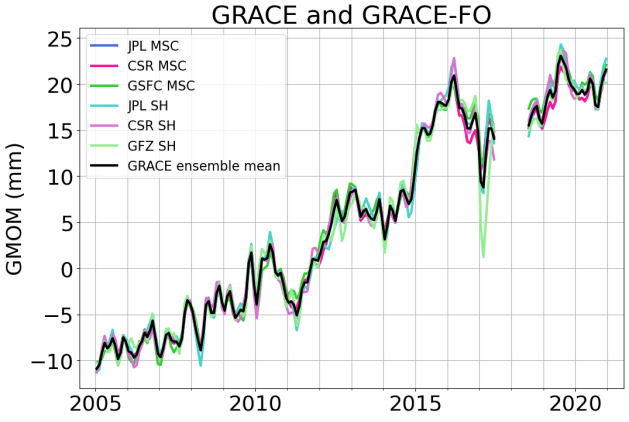

Figure 1. Global mean ocean mass time series from GRACE and GRACE-FO mascon (MSC) and spherical harmonics (SH) datasets. The black curve corresponds to the ensemble mean. Linear trends for all time series over different periods of time are provided in Table SI1.

Stoke's coefficients of the residual gravitational potential, corresponding to anomalies with respect to modelled atmospheric and ocean effects. The ocean mass change is obtained from the Stokes' coefficients by adding the GAB product to restore the modelled contribution of the dynamic ocean. The Glacial Isostatic Adjustment (GIA) effect is already corrected in the mascon data with the ICE6G-D model (Peltier et al., 2018). We remove the same GIA model from the spherical harmonics solutions. Corrections are also applied for the degree-1 (Swenson et al., 2008; Sun et al., 2016) and C20 (Loomis et al., 2020) coefficients. No spatial filtering is applied before computing the global mean time series in order to keep the total ocean mass constant.

The individual and ensemble mean GMOM time series based on GRACE and GRACE-FO data are shown in Figure 1. The GMOM time series display important interannual variability mostly related to the El Niño Southern Oscillation, in particular during the 2011 La Niña event (Fasullo et al., 2013) that caused a significant negative anomaly and the 2015 El Niño event that caused a positive anomaly. All six solutions agree well except in early 2017 where the spherical harmonics solutions appear significantly different from the mascon solutions. This might be due to a higher noise level in the GRACE data (e.g. Fig. 2 from Chen et al., 2022) especially at low degrees (e.g. abrupt changes in the C21 over mid-2016 to mid-2017, see for example Fig.7 from Dahle et al., 2019), better removed in mascon solutions using a spatially and temporally variable regularisation (e.g. Loomis et al., 2019). The difference between the mascon and spherical harmonics solutions is shown in Figure SI2. No trend difference is observed between the two types of solutions over 2005-2020.

The uncertainty associated with the GRACE and GRACE-FO GMOM time series is computed from the variance-covariance matrix of the ensemble of spherical harmonics solutions constructed by Blazquez et al. (2018) by varying the processing centres and corrections applied for the geocenter motion, Earth oblateness, filtering, leakage and GIA.

https://doi.org/10.5194/egusphere-2022-716
Preprint. Discussion started: 8 August 2022

3.2 Greenland and Antarctica ice sheet data

The amount of ice mass changes from Greenland and Antarctic ice sheets can be estimated from three independent approaches (e.g. Shepherd et al., 2012; Hanna et al., 2013; Cazenave and the WCRP Global Sea Level Budget Group, 2018): (1) volume change estimated using altimetry data, (2) mass change estimated from gravimetric data, and (3) mass change estimated by the input-output method (IOM) using the surface mass balance from models and the ice discharge measured by InSAR data.

In this study, we consider mostly IOM and altimetry products from different datasets to estimate ice sheet mass loss independently from GRACE and GRACE-FO data. For Greenland, we use: (1) IOM estimate from Velicogna et al. (2020), (2) multi-approach estimate from the Ice sheet Mass Balance Inter-comparison Exercise (IMBIE; Shepherd et al., 2021), (3) IOM estimate from Mankoff et al. (2021) and (4) altimetry estimate from Simonsen et al. (2021). For Antarctica, we use: (1) IOM estimate from Velicogna et al. (2020) and (2) multi-approach IMBIE estimate (Shepherd et al., 2021).

IMBIE provides a combination of estimates obtained from the three methods and provides an uncertainty estimate from the spread of the estimates. It is worth noting that the IMBIE product is not independent from GRACE and GRACE-FO data, however, in view of the good agreement between the gravimetric and the altimetric approaches (IMBIE, 2018, 2020; Otosaka, 2021), we choose to include these data in the global mean ocean mass budget assessment. Velicogna et al. (2020) compares and provides estimates from the IOM with trends adjusted using GRACE data (nevertheless independent from GRACE-FO data). Mankoff et al. (2021) provides IOM data for Greenland only. Simonsen et al. (2021) provides estimates based on altimetric data (using ERS-1, ERS-2, Envisat, CryoSat-2 and Sentinel-3 missions). To obtain the sea level contribution from ice mass change, we assume that water is evenly redistributed over the global ocean. Considering a global ocean surface of 361.4×10^8 km^2, 1 Gt of ice is equivalent to 1/361.4 mm of sea level change. In the following, we use ensemble mean time series from the above listed datasets, following the processing described in section 2.2. Figure 2 shows the time series of ocean mass contribution for the individual datasets as well as the ensemble means for Greenland and Antarctica. The ensemble means compared with a purely gravimetry estimate from Velicogna et al. (2020) shows that GRACE and GRACE-FO observations allow a better time sampling rate, hence allow capturing a stronger temporal variability (Figure SI3).

3.3 Land glaciers and ice caps data

To take into account the contribution of glaciers and ice caps to the ocean mass change, we use the recently published data from Hugonnet et al. (2021) covering the 2000-2019 period. The authors used the glacier outlines from the Global Land Ice Measurements from Space for the Caucasus Middle East region and from the Randolph Glacier Inventory 6.0 everywhere else. They computed the glacier elevation time series using the following satellite digital elevation models (DEM): ASTER, ArcticDEM and Reference Elevation Model of Antarctica (REMA). The volume change of each glacier was computed with a weighted mean local hypsometric method (McNabb et al., 2019; Hugonnet et al., 2021). For our study, we do not include Greenland glaciers as they are already taken into account in the Greenland ice sheet data (section 3.2).

https://doi.org/10.5194/egusphere-2022-716
Preprint. Discussion started: 8 August 2022

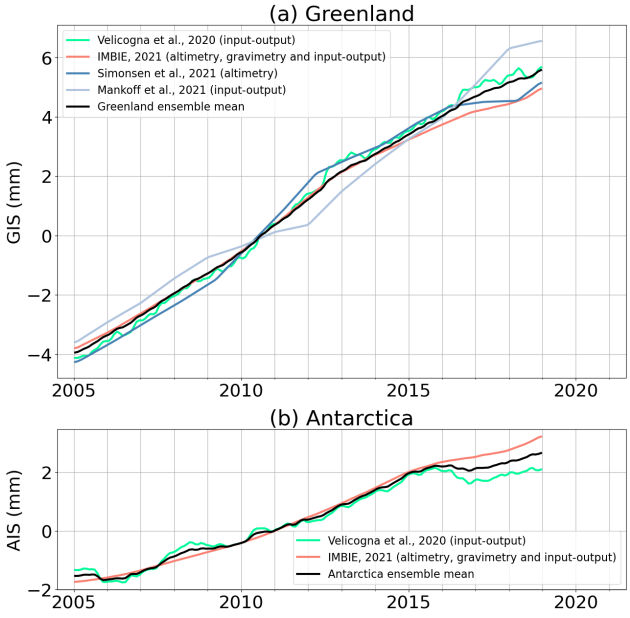

Figure 2. Contributions of (a) Greenland ice-sheet (GIS) and (b) Antarctica ice-sheet (AIS) melting to global mean ocean mass change. For each dataset, the method used to estimate the contribution (gravimetry, altimetry or input-output) is indicated in brackets. The black curves correspond to the ensemble means. Linear trends of all time series over different periods of time are provided in Table SI1.

3.4 Terrestrial water storage models

Water stored on land contributes to the changes in global mean ocean mass through the exchange of water between land and oceans. The total terrestrial water storage (TWS) variations result from the water content variations in different reservoirs on land: snow, canopy, soil moisture, groundwater, lakes, reservoirs, wetland and rivers. The change in water content of these reservoirs are driven both by the natural climate variability and by human activities (e.g. dams on rivers and groundwater abstraction). TWS variations can be estimated from GRACE and GRACE-FO data but here we use global hydrological models independent from gravimetric data.

We consider two hydrological models. The ISBA-CTRIP (Interaction Soil-Biosphere-Atmosphere, Total Runoff Integrating Pathways from the Centre National de Recherches Météorologiques) provides estimates until the end of 2018 (Decharme et al., 2010, 2019). The WaterGAP (Water Global Assessment and Prognosis) global hydrological model (WGHM) provides data until the end of 2016 (Döll et al., 2003, 2015; Müller Schmied et al., 2020; Müller Schmied et al., 2021). The WGHM provides four estimates of TWS, using two precipitation models and two assumptions on consumptive irrigation water use. The comparison of the ISBA-CTRIP and WGHM models is shown in Figure 3. Over 2005-2016, a trend difference of -0.41 $\pm$ 0.24 mm/yr is observed between the two models (Table SI1 and Figure 3b). This is likely due to the fact that, unlike WGHM, ISBA-CTRIP does not include the human-induced contributions (HIC) to the TWS estimate. The TWS HIC has become increasingly important over the last decades, reaching a trend of 0.37 (0.30 to 0.45) mm/yr (expressed in sea level equivalent)

https://doi.org/10.5194/egusphere-2022-716
Preprint. Discussion started: 8 August 2022

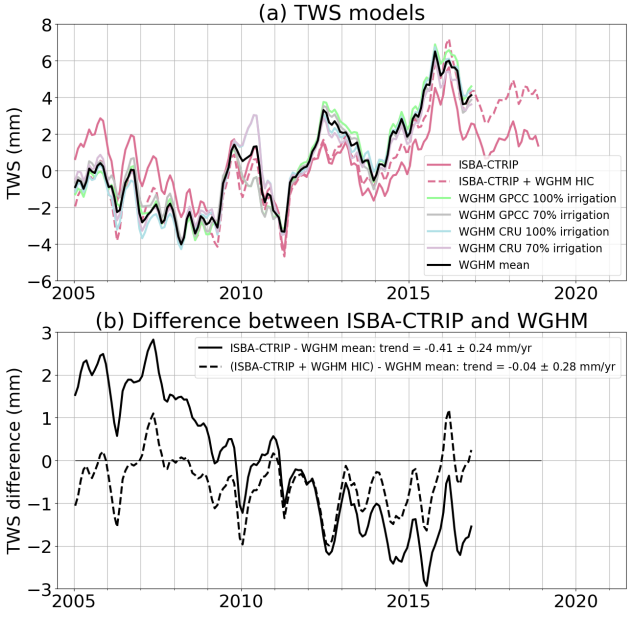

Figure 3. Comparison of ISBA-CTRIP and WGHM estimates of terrestrial water storage (TWS) variations. (a) ISBA-CTRIP and WGHM time series. The black curve corresponds to the mean of the four WGHM estimates. The red dotted curve corresponds to the sum of the ISBA-CTRIP climate contribution of the WGHM trend of human-induced contribution (HIC). (b) Difference between ISBA-CTRIP TWS and WGHM mean estimate of TWS. Linear trends of all time series over different periods of time are provided in Table SI1.

over 2003-2016 as estimated using WGHM by Cáceres et al. (2020). Adding this trend to ISBA-CTRIP TWS reduces the trend difference between the two models to -0.04 $\pm$ 0.28 mm/yr.

In this work, as we aim at understanding the non-closure of the budget after 2016, we use the ISBA-CTRIP model which provides data beyond 2016, and account for the TWC HIC trend estimated by Cáceres et al. (2020). As standard uncertainties, we assign the range of trends provided by Cáceres et al. (2020) over 2003-2016, i.e. 0.13 mm/yr for the climate-driven TWS and 0.15 mm/yr for the human-induced contribution.

3.5 Altimetry-based GMTSL data

We compute the GMSL time series from the vDT2021 sea level product operationally generated by the Copernicus Climate Change Service (C3S). This dataset is dedicated to the sea level stability for climate studies (Legeais et al., 2021). It provides daily sea level anomalies grids at a 1/4 degree spatial resolution from January 1993 until August 2021, based at any time on a reference altimeter mission (TOPEX/Poseidon, Jason-1, Jason-2, Jason-3 and Sentinel-6 Michaël Freilich), plus a complementary mission (ERS-1,2, Envisat, Cryosat or SARAL/AltiKa depending on the time frame) to increase the spatial coverage. The GMSL time series is corrected for the GIA effect considering a value of -0.3 $\pm$ 0.05 mm/yr (Peltier, 2004) as well as for the sea floor subsidence due to the present-day ice melting with a rate of -0.13 $\pm$ 0.01 mm/yr (Frederikse et al., 2017; Lickley

https://doi.org/10.5194/egusphere-2022-716
Preprint. Discussion started: 8 August 2022

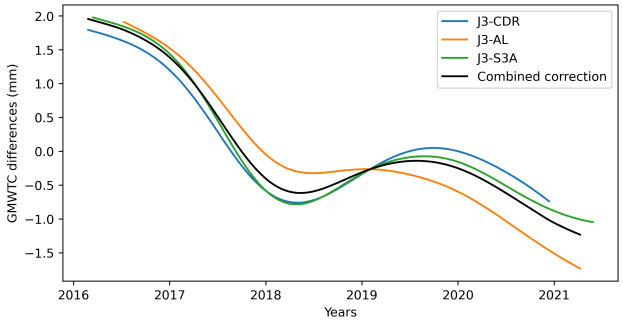

Figure 4. Differences between global mean wet tropospheric corrections (GMWTC) from Jason-3 (J3) microwave radiometer (MWR), derived from water vapour climate data records (CDRs), from SARAL/AltiKa (AL) MWR and from Sentinel-3A (S3A) MWR. The average (black curve) of these differences is used as empirical correction for the drift of Jason-3 radiometer.

et al., 2018). The GMSL and GMSL trend uncertainties are computed using the uncertainty budget and computational method detailed by Ablain et al. (2019).

Barnoud et al. (2022) showed that the wet tropospheric correction (WTC) derived from the microwave radiometer (MWR) instrument on-board the Jason-3 satellite, launched in 2016, is likely drifting. This drift was outlined from the comparison of Jason-3's radiometer WTC with a WTC derived from highly stable water vapour climate data records (Schröder et al., 2016) as well as with the radiometer's WTC from the SARAL/AltiKa and Sentinel-3A altimetry missions (Barnoud et al., 2022, In preparation). The Jason-3 radiometer drift is estimated from the global mean WTC differences between Jason-3, SARAL/AltiKa, Sentinel-3A and the climate data records (Figure 4). The global mean WTC differences show similar low frequency variations. An overall trend of -0.5 mm/yr is observed, but most of the drift is occurring during the first two years of the Jason-3 mission. We compute the average of the three global mean WTC differences that we use as correction for the GMSL over the Jason-3 period.

3.6 Thermosteric sea level data

The global mean thermosteric sea level (GMTSL) is computed from seven in-situ oceanographic datasets: (a) EN4.2.2 data from the Met Office Hadley Center (Good et al., 2013) with Gouretski and Reseghetti (2010) correction applied, (b) IAP (Institute of Atmospheric Physics from the Chinese Academy of Sciences) data (Cheng et al., 2017, 2020), (c) the IFREMER (Institut Français de Recherche pour l'Exploitation de la Mer) ISAS (In Situ Analysis System) 20 dataset (Gaillard et al., 2016), (d) Ishii et al. (2017) data, (e) JAMSTEC (Japan Agency for Marine-Earth Science and Technology) MOAA GPV (Grid Point Value of the Monthly Objective Analysis using the Argo data) version 2021 product data set (Hosoda et al., 2010), (f) NOAA (National Oceanic and Atmospheric Administration) data (Levitus et al., 2012; Garcia et al., 2019) and (g) SIO (Scripps Institute of Oceanography) data (Roemmich and Gilson, 2009). The seven datasets are mainly based on Argo data

https://doi.org/10.5194/egusphere-2022-716
Preprint. Discussion started: 8 August 2022

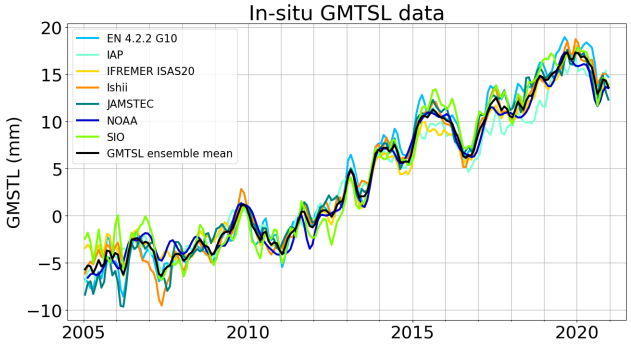

Figure 5. Global mean thermosteric sea level (GMTSL) variations time series from the seven datasets used in this study. The black curve corresponds to the ensemble mean. Linear trends of all time series over different periods of time are provided in Table SI1.

(Argo, 2021). In addition, EN4 and IAP datasets also include MBT and XBT data. JAMSTEC includes Triangle Trans-Ocean Buoy Network (TRITON) data and additional conductivity-temperature-depth profiler data from ships.

From these datasets, we compute the thermosteric sea level change due to temperature variations between 0 and 2000 m depth. A linear trend of 0.12 ± 0.03 mm/yr is added to the GMTSL to take into account the contribution of the deep ocean (Chang et al., 2019). Figure 5 shows the individual GMTSL time series as well as the ensemble mean.

4 Resulting global mean ocean mass budgets

4.1 Budget from the sum of mass contributions

Figure 6a shows the ocean mass budget comparing the GRACE-based GMOM to the sum of its contributions from ice sheets, ice caps, glaciers and terrestrial water storage. The budget residuals are shown in Figure 6b. The drop in the gravimetry-based GMOM in early 2017 is linked to the processing of spherical harmonic solutions and does not appear when using mascon solutions only as shown in Figures SI2 and SI4. No significant residual trend is observed over 2005-2018, but a significant negative residual trend estimated at -1.60 ± 0.36 mm/yr is observed over 2015-2018 (Table SI1). This residual trend could be due to an underestimation of the gravimetry-based GMOM as well as to an overestimation of the freshwater input by the land ice and water storage variation models or neglected contribution from the atmospheric water vapour for instance.

4.2 Comparing with the altimetry-based GMSL corrected for the thermal expansion

We also compare the gravimetry-based GMOM to the altimetry-based GMSL corrected for the thermal expansion using in-situ oceanographic data. Results are shown in Figure 7a with and without correcting Jason-3 altimetry data for the WTC of Jason-3 MWR drift as of 2016. Correcting for the Jason-3 WTC drift (Figure 7, dotted lines), the budget residual trend amounts to -0.38 ± 0.22 mm/yr over 2005-2020 and -0.96 ± 0.48 mm/yr over 2015-2020. The budget residual trend is reduced by about 40 % beyond 2015 compared to the case where no Jason-3 WTC drift correction is applied (residual trend of -0.52 ± 0.22 mm/yr

https://doi.org/10.5194/egusphere-2022-716
Preprint. Discussion started: 8 August 2022

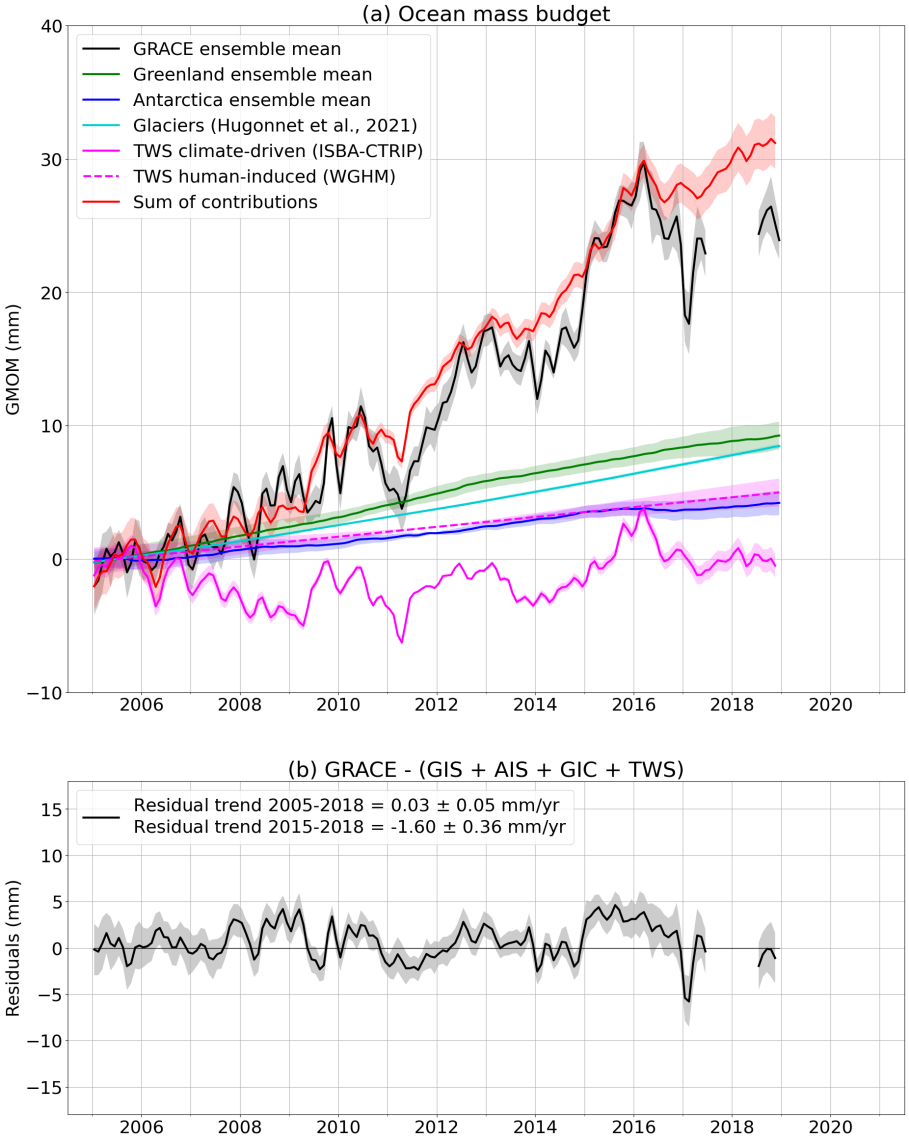

Figure 6. Ocean mass budget. (a) Budget with GRACE/GRACE-FO based global mean ocean mass (GMOM) variations and the sum of its contributions from Greenland (GIS), Antarctica (AIS), land glaciers (GIC) and terrestrial water storage (TWS) variations. TWS variations are split into the climate-driven component from ISBA-CTRIP and the human-induced contribution trend estimated from WGHM (Cáceres et al., 2020). (b) Budget residuals. Linear trends of all components over different periods of time are provided in Table SI1.

over 2005-2020 and -1.52 ± 0.45 mm/yr over 2015-2020). Although this is a significant improvement, the empirical Jason-3 WTC drift correction does not allow closing the mass budget within uncertainties, leaving an unexplained residual drift beyond 2015. This important issue needs further investigations.

https://doi.org/10.5194/egusphere-2022-716
Preprint. Discussion started: 8 August 2022

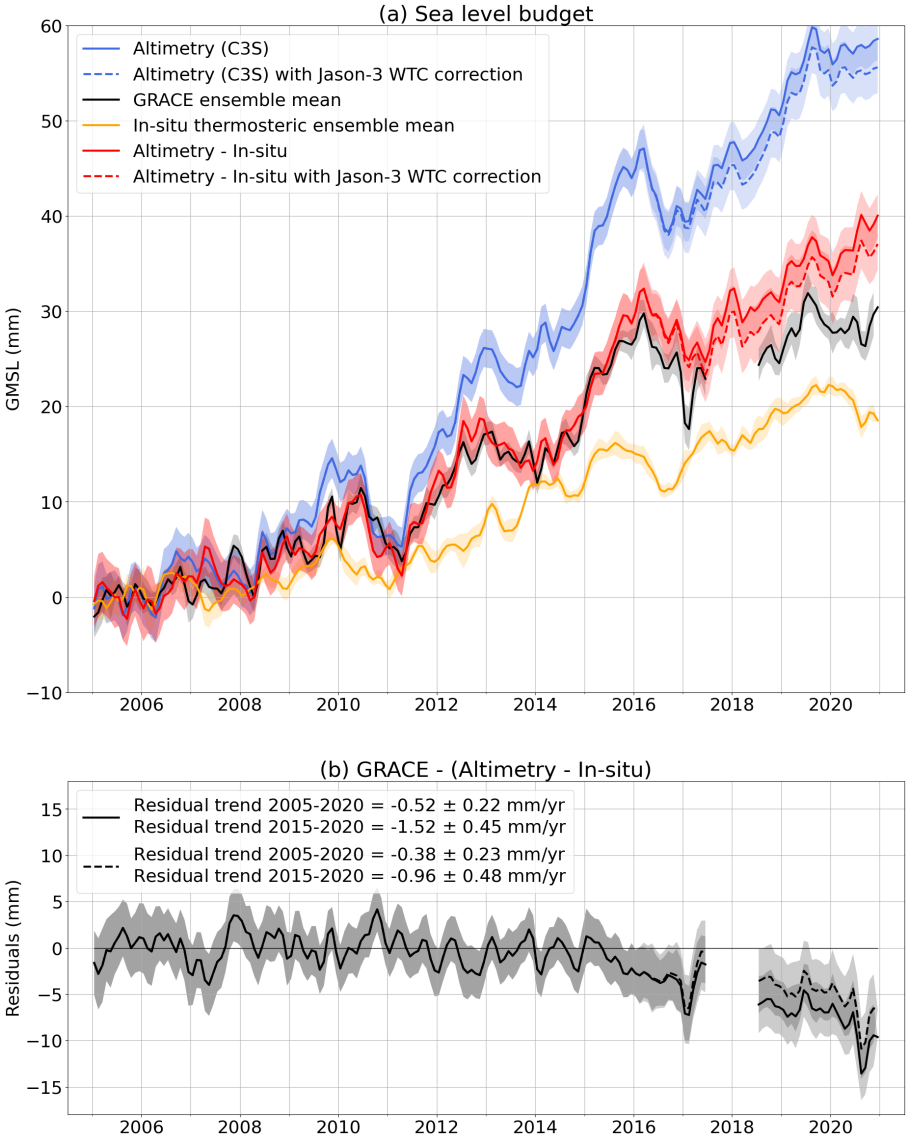

Figure 7. Sea level budget. (a) Budget with GRACE/GRACE-FO based global mean ocean mass (GMOM) variations compared to altimetry-based GMSL and Argo-based GMTSL. (b) Budget residuals. The budget and residuals are assessed without (solid lines) and with (dashed lines) correcting for the Jason-3 radiometer drift. Linear trends of all components over different periods of time are provided in Table SI1.

4.3 Discussion

In section 4, we compared the GRACE and GRACE-FO based GMOM to the sum of the individual ocean mass contributions (section 4.1) and to the GMSL corrected for thermal expansion and for Jason-3 WTC drift (section 4.2). We found that the GMOM budget residuals show significant trends of -1.60 ± 0.36 mm/yr over 2015-2018 with respect to the individual ocean

https://doi.org/10.5194/egusphere-2022-716
Preprint. Discussion started: 8 August 2022

mass contributions and of -0.96 ± 0.48 mm/yr over 2015-2020 with respect to the altimetry corrected for the thermal expansion. Note that we compute linear trends to quantify the non-closure. However, over such short time spans, we cannot exclude that the residuals mostly result from interannual signals (instead of linear trends) not well accounted for by the data used to estimate the components of the budgets. For completeness, the altimetry-based GMSL corrected for Jason-3 WTC drift is also compared to the sum of the thermal expansion and of the individual ocean mass contributions (Figure 8). This is an alternative budget of sea level, independent of GRACE and GRACE-FO. Nevertheless, the residual time series still displays significant interannual variability, especially between 2015 and 2017 (Figure 8b). This means that the gravimetry-based GMOM cannot be fully responsible for the non-closure of the ocean mass budget observed over the last few years. In an effort to understand the causes of the remaining non-closure, we compare the residuals of the budgets assessed in this study (Figure 9). We have estimated three types of budget residuals: (i) the gravimetry-based GMOM minus the sum of the altimetry-based GMSL corrected for the thermal expansion and for Jason-3 WTC drift, (ii) the gravimetry-based GMOM minus the sum of the individual mass contributions, and (iii) the altimetry-based GMSL minus the thermal expansion and the individual mass contributions. In Figure 9, we compare the residuals related to the gravimetry-based GMOM (Figure 9a), to the altimetry-GMSL corrected for the thermal expansion and for Jason-3 radiometer drift (Figure 9b) and to the land ice and water storage models (Figure 9c). Residual time series involving the GRACE and GRACE-FO-based GMOM corrected either with the sum of mass contributions or with the GMSL corrected for the thermal expansion both exhibit a significant negative linear trend over 2015-2018. The gravimetry-based GMOM might be partly responsible for this non-closure. However, significant residuals also occur when computing the residuals of the budget without using the GRACE and GRACE-FO based GMOM (Fig 8c). While the linear trend is lower (-0.81 ± 0.39 mm/yr), significant interannual variability is observed in the residuals around 2015-2017 (Fig. 8c). Such residuals could be due to issues in altimetry or steric data, or in the land ice and water storage models. In particular, high uncertainties are linked with the TWS variations provided by the hydrological models, as shown in section 3.4.

The ocean mass budgets show that GRACE and GRACE-FO data may explain part of the non-closure. Kim et al. (2021) explains that the different GIA and degree 1 models used to correct GRACE and GRACE-FO data lead to uncertainties on the trends. This effect should be encompassed in the GMOM uncertainty estimated from Blazquez et al. (2018) that we use in the present study. On the other hand, the significant residuals in the sea level budget calculated independently from GRACE and GRACE-FO show that they cannot be fully responsible for the non-closure. A possible explanation is that the budget neglects some contributions such as the evolution of the deep ocean below 2000 m depth, the atmospheric water vapour variations and the permafrost thawing. While neglected until recently (e.g. Horwath et al., 2022), these components may have a growing contribution to the mass budget.

5 Conclusions

The global mean ocean mass budget comparing the GRACE and GRACE-FO estimate to the sum of individual mass contributions (ice mass changes from ice sheets, ice caps and glaciers and terrestrial water storage variations) shows a significant residual trend of -1.60 ± 0.36 mm/yr over 2015-2018. We show that a drift of Jason-3 WTC is responsible for about 40 %

https://doi.org/10.5194/egusphere-2022-716
Preprint. Discussion started: 8 August 2022

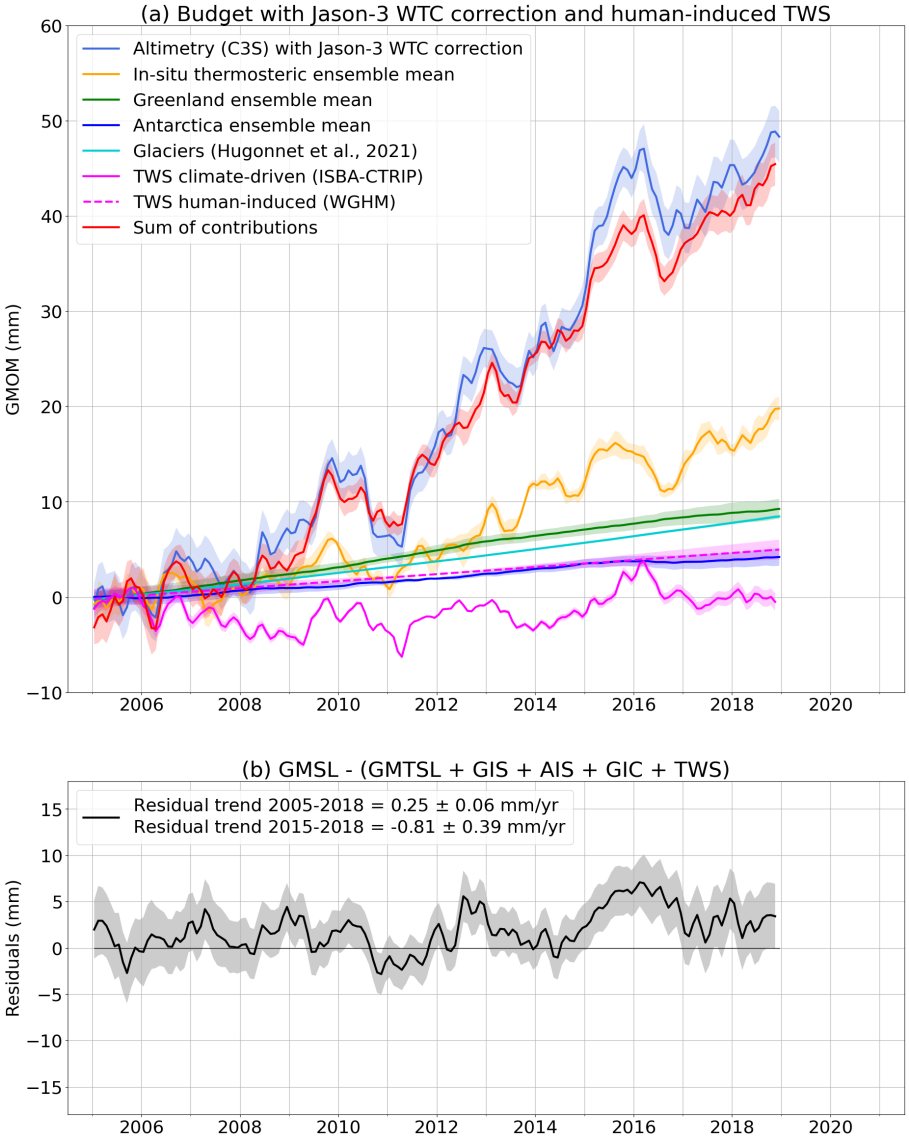

Figure 8. Sea level budget using the individual ocean mass contributions. (a) Initial unclosed sea level budget. (b) Initial budget residuals. (c) Updated sea level budget taking into account Jason-3 radiometer drift correction and human-induced TWS contribution. (d) Updated budget residuals. Linear trends of all components over different periods of time are provided in Table SI1.

of the non-closure of the budget beyond 2015 when comparing the GMOM to the altimetry-based GMSL corrected for the thermal expansion. A correction for Jason-3 WTC drift is estimated based on the WTC from water vapour climate data records as well as from SARAL/AltiKa and Sentinel-3A altimetry missions. After applying this correction, a significant residual trend of -0.96 ± 0.48 mm/yr over 2015-2020 is left in the budget. Finally, the sea level budget comparing the altimetry-based GMSL corrected for the thermal extension with the sum of the individual mass contributions leads to significant interannual variability

https://doi.org/10.5194/egusphere-2022-716
Preprint. Discussion started: 8 August 2022

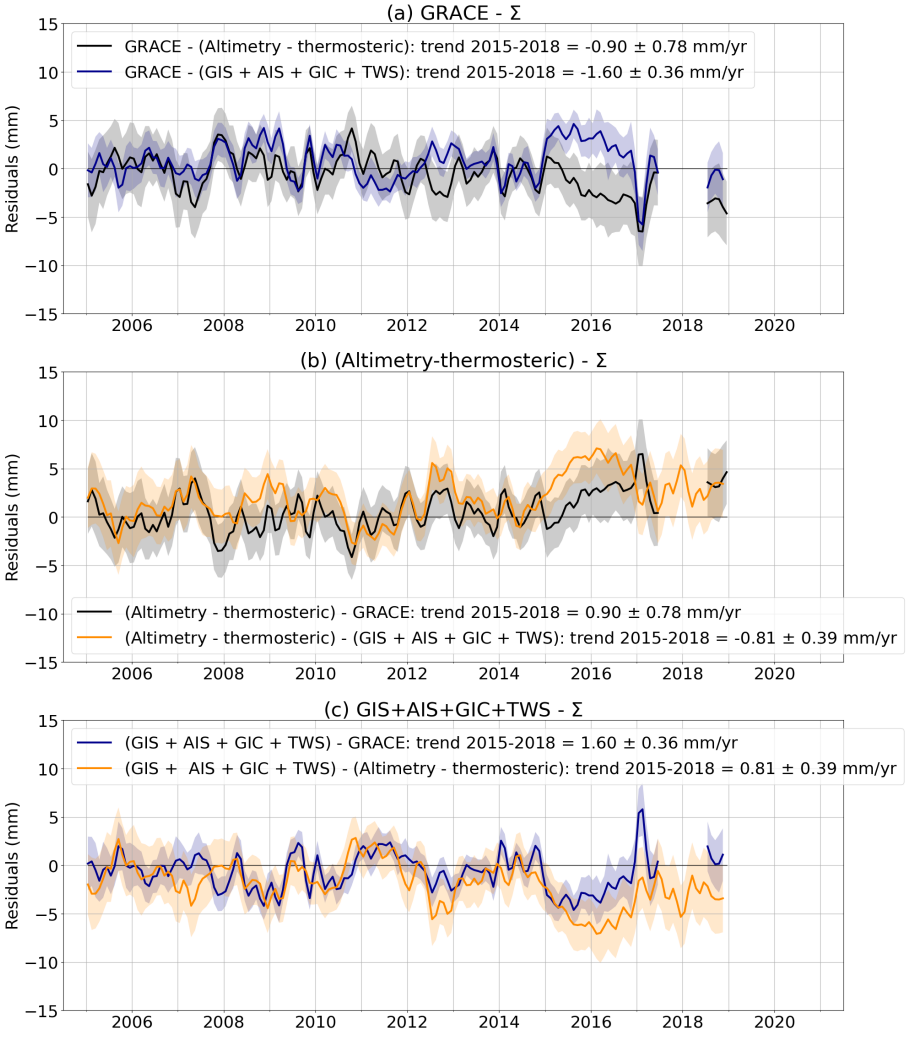

Figure 9. Comparison of the residual time series from the budgets shown in Figures 6, 7 and 8. (a) Residuals time series involving the GRACE and GRACE-FO-based GMOM. (b) Residual time series with respect to the altimetry-based GMSL corrected for thermal expansion. (c) Residual time series with respect to the models of land ice and water storage variations.

in the residuals around 2015-2017. Because the latter budget was calculated independently from gravimetric data, GRACE and GRACE-FO data cannot be fully responsible for the non-closure of the ocean mass budget. Further improving the budget closure after 2016 involves investigating unidentified errors in other components (thermosteric sea level, deep ocean contribution, neglected components such as the permafrost thawing or the atmospheric water content variations). Assessing the ocean mass budget at regional scale might also help identify patterns and understand processes responsible for the non-closure at global scale.

https://doi.org/10.5194/egusphere-2022-716
Preprint. Discussion started: 8 August 2022

Data availability. The GRACE/GRACE Follow-On JPL, CSR and GFZ Level 2 (Stock's coefficients) and Level 3 (mascon) Release 6 data are available from https://podaac.jpl.nasa.gov. The GRACE/GRACE Follow-On GSFC data are available from https://earth.gsfc.nasa.gov/geo/data/grace-mascons. The C3S altimetry data are available from https://cds.climate.copernicus.eu/cdsapp#!/dataset/satellite-sea-level-global?tab=overview. The AVISO altimetry along-track data for Jason-3, SARAL/AltiKa and Sentinel-3A are available from https://www.aviso.altimetry.fr/. The total column water vapour REMSS climate data records are available at https://wui.cmsaf.eu/safira/action/viewProduktDetails?eid=21864&fid=23. Argo data were collected and made freely available by the international Argo Program and the national programs that contribute to it (https://argo.ucsd.edu, https://www.ocean-ops.org). The Argo Program is part of the Global Ocean Observing System. The NOAA Argo data are available from https://www.ncei.noaa.gov/access/global-ocean-heat-content/. The SIO Argo climatology data are available from http://sio-argo.ucsd.edu/RG_Climatology.html. The JAMSTEC MOAA GPV data are available from http://www.jamstec.go.jp/ARGO/argo_web/argo/?page_id=83&lang=en. The EN4 Argo data are available from http://hadobs.metoffice.com/en4/download.html. The IAP data are available from http://159.226.119.60/cheng/. The IFREMER ISAS20 data are available from https://www.seanoe.org/data/00412/52367/. The Ishii v7.3.1 data are available from https://climate.mri-jma.go.jp/pub/ocean/ts/v7.3.1/. The TWS WGHM v2.2d data are available from https://doi.pangaea.de/10.1594/PANGAEA.918447?format=html#download. The TWS ISBA-CTRIP data are available from the authors (Decharme et al., 2019). For Greenland, Antarctica and glaciers datasets, we invite the reader to refer to the references cited in the article and the links provided therein.

Author contributions. AB conducted the study and wrote the initial version of the manuscript. AC supervised the work. JP and MA participated in the discussion of the results. All authors have read, improved and agreed with the content of the manuscript.

Competing interests. The authors declare no conflict of interests.

Acknowledgements. The research leading to these results has received funding from the European Research Council (ERC) under the European Union's Horizon 2020 research and innovation program (GRACEFUL Synergy Grant agreement No 855677).

https://doi.org/10.5194/egusphere-2022-716
Preprint. Discussion started: 8 August 2022

References

Ablain, M., Meyssignac, B., Zawadzki, L., Jugier, R., Ribes, A., Spada, G., Benveniste, J., Cazenave, A., and Picot, N.: Uncertainty in satellite estimates of global mean sea-level changes, trend and acceleration, Earth System Science Data, 11, 1189–1202, https://doi.org/10.5194/essd-11-1189-2019, 2019.

Argo: Argo float data and metadata from Global Data Assembly Centre (Argo GDAC), https://doi.org/10.17882/42182, 2021.

Bandikova, T., McCullough, C., Kruizinga, G. L., Save, H., and Christophe, B.: GRACE accelerometer data transplant, Advances in Space Research, 64, 623–644, https://doi.org/10.1016/j.asr.2019.05.021, 2019.

Barnoud, A., Pfeffer, J., Guérou, A., Frery, M.-L., Siméon, M., Cazenave, A., Chen, J., Llovel, W., Thierry, V., Legeais, J.-F., and Ablain, M.: Contributions of altimetry and Argo to non-closure of the global mean sea level budget since 2016, Geophysical Research Letters, https://doi.org/10.1029/2021gl092824, 2021.

Barnoud, A., Picard, B., Meyssignac, B., Marti, F., Ablain, M., and Roca, R.: Reducing uncertainties of global mean sea level, global ocean heat content and Earth's energy imbalance using water vapour climate data records, in: Sea level worshop, Brest, France, 2022.

Barnoud, A., Picard, B., Meyssignac, B., Marti, F., Ablain, M., and Roca, R.: Reducing the long term uncertainties of global mean sea level trend using highly stable water vapour climate data records, In preparation.

Bettadpur, S.: Gravity Recovery and Climate Experiment Level-2 Gravity Field Product User Handbook, Tech. rep., Center for Space Research at The University of Texas at Austin, https://podaac-tools.jpl.nasa.gov/drive/files/allData/grace/docs/L2-UserHandbook_v4.0.pdf, 2018.

Blazquez, A., Meyssignac, B., Lemoine, J., Berthier, E., Ribes, A., and Cazenave, A.: Exploring the uncertainty in GRACE estimates of the mass redistributions at the Earth surface: implications for the global water and sea level budgets, Geophysical Journal International, 215, 415–430, https://doi.org/10.1093/gji/ggy293, 2018.

Cáceres, D., Marzeion, B., Malles, J. H., Gutknecht, B. D., Schmied, H. M., and Döll, P.: Assessing global water mass transfers from continents to oceans over the period 1948–2016, Hydrology and Earth System Sciences, 24, 4831–4851, https://doi.org/10.5194/hess-24-4831-2020, 2020.

Cazenave, A. and the WCRP Global Sea Level Budget Group: Global sea-level budget 1993–present, Earth System Science Data, 10, 1551–1590, https://doi.org/10.5194/essd-10-1551-2018, 2018.

Chang, L., Tang, H., Wang, Q., and Sun, W.: Global thermosteric sea level change contributed by the deep ocean below 2000 m estimated by Argo and CTD data, Earth and Planetary Science Letters, 524, 115 727, https://doi.org/10.1016/j.epsl.2019.115727, 2019.

Chen, J., Tapley, B., Seo, K.-W., Wilson, C., and Ries, J.: Improved Quantification of Global Mean Ocean Mass Change Using GRACE Satellite Gravimetry Measurements, Geophysical Research Letters, 46, 13 984–13 991, https://doi.org/10.1029/2019gl085519, 2019.

Chen, J., Tapley, B., Wilson, C., Cazenave, A., Seo, K.-W., and Kim, J.-S.: Global ocean mass change from GRACE and GRACE Follow-On and altimeter and Argo measurements, Geophysical Research Letters, 47, e2020GL090 656, https://doi.org/10.1029/2020GL090656, 2020.

Chen, J., Cazenave, A., Dahle, C., Llovel, W., Panet, I., Pfeffer, J., and Moreira, L.: Applications and Challenges of GRACE and GRACE Follow-On Satellite Gravimetry, Surveys in Geophysics, https://doi.org/10.1007/s10712-021-09685-x, 2022.

Cheng, L., Trenberth, K. E., Fasullo, J., Boyer, T., Abraham, J., and Zhu, J.: Improved estimates of ocean heat content from 1960 to 2015, Science Advances, 3, https://doi.org/10.1126/sciadv.1601545, 2017.

https://doi.org/10.5194/egusphere-2022-716
Preprint. Discussion started: 8 August 2022

Cheng, L., Trenberth, K. E., Gruber, N., Abraham, J. P., Fasullo, J. T., Li, G., Mann, M. E., Zhao, X., and Zhu, J.: Improved Estimates of Changes in Upper Ocean Salinity and the Hydrological Cycle, Journal of Climate, 33, 10 357–10 381, https://doi.org/10.1175/jcli-d-20-0366.1, 2020.

Dahle, C., Flechtner, F., Murböck, M., Michalak, G., Neumayer, H., Abrykosov, O., Reinhold, A., and König, R.: GRACE Geopotential GSM Coefficients GFZ RL06, https://doi.org/10.5880/GFZ.GRACE_06_GSM, 2018.

Dahle, C., Murböck, M., Flechtner, F., Dobslaw, H., Michalak, G., Neumayer, K., Abrykosov, O., Reinhold, A., König, R., Sulzbach, R., and Förste, C.: The GFZ GRACE RL06 Monthly Gravity Field Time Series: Processing Details and Quality Assessment, Remote Sensing, 11, 2116, https://doi.org/10.3390/rs11182116, 2019.

Decharme, B., Alkama, R., Douville, H., Becker, M., and Cazenave, A.: Global Evaluation of the ISBA-TRIP Continental Hydrological System. Part II: Uncertainties in River Routing Simulation Related to Flow Velocity and Groundwater Storage, Journal of Hydrometeorology, 11, 601–617, https://doi.org/10.1175/2010jhm1212.1, 2010.

Decharme, B., Delire, C., Minvielle, M., Colin, J., Vergnes, J.-P., Alias, A., Saint-Martin, D., Séférian, R., Sénési, S., and Voldoire, A.: Recent Changes in the ISBA-CTRIP Land Surface System for Use in the CNRM-CM6 Climate Model and in Global Off-Line Hydrological Applications, Journal of Advances in Modeling Earth Systems, 11, 1207–1252, https://doi.org/10.1029/2018ms001545, 2019.

Dobslaw, H., Bergmann-Wolf, I., Dill, R., Poropat, L., Thomas, M., Dahle, C., Esselborn, S., König, R., and Flechtner, F.: A new high-resolution model of non-tidal atmosphere and ocean mass variability for de-aliasing of satellite gravity observations: AOD1B RL06, Geophysical Journal International, 211, 263–269, https://doi.org/10.1093/gji/ggx302, 2017.

Dobslaw, H., Dill, R., Bagge, M., Klemann, V., Boergens, E., Thomas, M., Dahle, C., and Flechtner, F.: Gravitationally Consistent Mean Barystatic Sea Level Rise From Leakage-Corrected Monthly GRACE Data, Journal of Geophysical Research: Solid Earth, 125, https://doi.org/10.1029/2020jb020923, 2020.

Döll, P., Kaspar, F., and Lehner, B.: A global hydrological model for deriving water availability indicators: model tuning and validation, Journal of Hydrology, 270, 105–134, https://doi.org/10.1016/s0022-1694(02)00283-4, 2003.

Döll, P., Douville, H., Güntner, A., Schmied, H. M., and Wada, Y.: Modelling Freshwater Resources at the Global Scale: Challenges and Prospects, Surveys in Geophysics, 37, 195–221, https://doi.org/10.1007/s10712-015-9343-1, 2015.

Fasullo, J. T., Boening, C., Landerer, F. W., and Nerem, R. S.: Australia's unique influence on global sea level in 2010-2011, Geophysical Research Letters, 40, 4368–4373, https://doi.org/10.1002/grl.50834, 2013.

Frederikse, T., Simon, K., Katsman, C. A., and Riva, R.: The sea-level budget along the N orthwest A tlantic coast: GIA , mass changes, and large-scale ocean dynamics, Journal of Geophysical Research: Oceans, 122, 5486–5501, https://doi.org/10.1002/2017jc012699, 2017.

Gaillard, F., Reynaud, T., Thierry, V., Kolodziejczyk, N., and von Schuckmann, K.: In Situ–Based Reanalysis of the Global Ocean Temperature and Salinity with ISAS: Variability of the Heat Content and Steric Height, Journal of Climate, 29, 1305–1323, https://doi.org/10.1175/jcli-d-15-0028.1, 2016.

Garcia, H. E., Boyer, T. P., Baranova, O. K., Locarnini, R. A., Mishonov, A. V., Grodsky, A., Paver, C. R., Weathers, K. W., Smolyar, I. V., Reagan, J. R., Seidov, D., and Zweng, M. M.: World Ocean Atlas 2018: Product Documentation, Tech. rep., NOAA, https://data.nodc.noaa.gov/woa/WOA18/DOC/woa18documentation.pdf, mishonov, A., Technical Editor., 2019.

Good, S. A., Martin, M. J., and Rayner, N. A.: EN4: Quality controlled ocean temperature and salinity profiles and monthly objective analyses with uncertainty estimates, Journal of Geophysical Research: Oceans, 118, 6704–6716, https://doi.org/10.1002/2013jc009067, 2013.

https://doi.org/10.5194/egusphere-2022-716
Preprint. Discussion started: 8 August 2022

Gouretski, V. and Reseghetti, F.: On depth and temperature biases in bathythermograph data: Development of a new correction scheme based on analysis of a global ocean database, Deep Sea Research Part I: Oceanographic Research Papers, 57, 812–833, https://doi.org/10.1016/j.dsr.2010.03.011, 2010.

Gregory, J. M. and Lowe, J. A.: Predictions of global and regional sea-level rise using AOGCMs with and without flux adjustment, Geophysical Research Letters, 27, 3069–3072, https://doi.org/10.1029/1999gl011228, 2000.

Hakuba, M. Z., Frederikse, T., and Landerer, F. W.: Earth's Energy Imbalance From the Ocean Perspective (2005–2019), Geophysical Research Letters, 48, https://doi.org/10.1029/2021gl093624, 2021.

Hanna, E., Navarro, F. J., Pattyn, F., Domingues, C. M., Fettweis, X., Ivins, E. R., Nicholls, R. J., Ritz, C., Smith, B., Tulaczyk, S., Whitehouse, P. L., and Zwally, H. J.: Ice-sheet mass balance and climate change, Nature, 498, 51–59, https://doi.org/10.1038/nature12238, 2013.

Horwath, M., Gutknecht, B. D., Cazenave, A., Palanisamy, H. K., Marti, F., Marzeion, B., Paul, F., Bris, R. L., Hogg, A. E., Otosaka, I., Shepherd, A., Döll, P., Cáceres, D., Schmied, H. M., Johannessen, J. A., Nilsen, J. E. Ø., Raj, R. P., Forsberg, R., Sørensen, L. S., Barletta, V. R., Simonsen, S. B., Knudsen, P., Andersen, O. B., Randall, H., Rose, S. K., Merchant, C. J., Macintosh, C. R., von Schuckmann, K., Novotny, K., Groh, A., Restano, M., and Benveniste, J.: Global sea-level budget and ocean-mass budget, with focus on advanced data products and uncertainty characterisation, Earth Systems Science Data, 14, 411–447, https://doi.org/10.5194/essd-14-411-2022, 2022.

Hosoda, S., Ohira, T., Sato, K., and Suga, T.: Improved description of global mixed-layer depth using Argo profiling floats, Journal of Oceanography, 66, 773–787, https://doi.org/10.1007/s10872-010-0063-3, 2010.

Hugonnet, R., McNabb, R., Berthier, E., Menounos, B., Nuth, C., Girod, L., Farinotti, D., Huss, M., Dussaillant, I., Brun, F., and Kääb, A.: Accelerated global glacier mass loss in the early twenty-first century, Nature, 592, 726–731, https://doi.org/10.1038/s41586-021-03436-z, 2021.

IMBIE: Mass balance of the Antarctic Ice Sheet from 1992 to 2017, Nature, 558, 219–222, https://doi.org/10.1038/s41586-018-0179-y, 2018.

IMBIE: Mass balance of the Greenland Ice Sheet from 1992 to 2018, Nature, 579, 233–239, https://doi.org/10.1038/s41586-019-1855-2, 2020.

IPCC: IPCC Special Report on the ocean and cryosphere in a changing climate, Cambridge University Press, https://doi.org/10.1017/9781009157964, 2019.

Ishii, M., Fukuda, Y., Hirahara, S., Yasui, S., Suzuki, T., and Sato, K.: Accuracy of Global Upper Ocean Heat Content Estimation Expected from Present Observational Data Sets, SOLA, 13, 163–167, https://doi.org/10.2151/sola.2017-030, 2017.

Kim, J.-S., Seo, K.-W., Chen, J., and Wilson, C.: Assessment of GRACE/GRACE Follow-On Estimates of Global Mean Ocean Mass Change, Resesarch Square, p. preprint, https://doi.org/10.21203/rs.3.rs-1182933/v1, 2021.

Landerer, F. W., Flechtner, F. M., Save, H., Webb, F. H., Bandikova, T., Bertiger, W. I., Bettadpur, S. V., Byun, S. H., Dahle, C., Dobslaw, H., Fahnestock, E., Harvey, N., Kang, Z., Kruizinga, G. L. H., Loomis, B. D., McCullough, C., Murböck, M., Nagel, P., Paik, M., Pie, N., Poole, S., Strekalov, D., Tamisiea, M. E., Wang, F., Watkins, M. M., Wen, H.-Y., Wiese, D. N., and Yuan, D.-N.: Extending the Global Mass Change Data Record: GRACE Follow-On Instrument and Science Data Performance, Geophysical Research Letters, 47, https://doi.org/10.1029/2020gl088306, 2020.

Legeais, J.-F., Meyssignac, B., Faugère, Y., Guerou, A., Ablain, M., Pujol, M.-I., Dufau, C., and Dibarboure, G.: Copernicus Sea Level Space Observations: A Basis for Assessing Mitigation and Developing Adaptation Strategies to Sea Level Rise, Frontiers in Marine Science, 8, https://doi.org/10.3389/fmars.2021.704721, 2021.

https://doi.org/10.5194/egusphere-2022-716
Preprint. Discussion started: 8 August 2022

Levitus, S., Antonov, J. I., Boyer, T. P., Baranova, O. K., Garcia, H. E., Locarnini, R. A., Mishonov, A. V., Reagan, J. R., Seidov, D., Yarosh, E. S., and Zweng, M. M.: World ocean heat content and thermosteric sea level change (0-2000 m), 1955-2010, Geophysical Research Letters, 39, n/a–n/a, https://doi.org/10.1029/2012gl051106, 2012.

Lickley, M. J., Hay, C. C., Tamisiea, M. E., and Mitrovica, J. X.: Bias in Estimates of Global Mean Sea Level Change Inferred from Satellite Altimetry, Journal of Climate, 31, 5263–5271, https://doi.org/10.1175/jcli-d-18-0024.1, 2018.

Llovel, W., Purkey, S., Meyssignac, B., Blazquez, A., Kolodziejczyk, N., and Bamber, J.: Global ocean freshening, ocean mass increase and global mean sea level rise over 2005–2015, Scientific Reports, 9, https://doi.org/10.1038/s41598-019-54239-2, 2019.

Loomis, B. D., Rachlin, K. E., and Luthcke, S. B.: Improved Earth Oblateness Rate Reveals Increased Ice Sheet Losses and Mass-Driven Sea Level Rise, Geophysical Research Letters, 46, 6910–6917, https://doi.org/10.1029/2019gl082929, 2019.

Loomis, B. D., Rachlin, K. E., Wiese, D. N., Landerer, F. W., and Luthcke, S. B.: Replacing GRACE/GRACE-FO With Satellite Laser Ranging: Impacts on Antarctic Ice Sheet Mass Change, Geophysical Research Letters, 47, https://doi.org/10.1029/2019gl085488, 2020.

Mankoff, K. D., Fettweis, X., Langen, P. L., Stendel, M., Kjledsen, K. K., Karlsson, N. B., Noël, B., van den Broeke, M. R., Colgan, W., Simonsen, S. B., Box, J. E., Solgaard, A., Ahlstrøm, A. P., Andersen, S. B., and Fausto, R. S.: Greenland ice sheet mass balance from 1840 through next week, Earth System Science Data, 13, 5001–5025, https://doi.org/10.5194/essd-13-5001-2021, 2021.

Marti, F., Blazquez, A., Meyssignac, B., Ablain, M., Barnoud, A., Fraudeau, R., Jugier, R., Chenal, J., Larnicol, G., Pfeffer, J., Restano, M., and Benveniste, J.: Monitoring the ocean heat content change and the Earth energy imbalance from space altimetry and space gravimetry, Earth System Science Data, https://doi.org/10.5194/essd-2021-220, 2022.

McNabb, R., Nuth, C., Kääb, A., and Girod, L.: Sensitivity of glacier volume change estimation to DEM void interpolation, The Cryosphere, 13, 895–910, https://doi.org/10.5194/tc-13-895-2019, 2019.

Müller Schmied, H., Cáceres, D., Eisner, S., Flörke, M., Herbert, C., Niemann, C., Peiris, T. A., Popat, E., Portmann, F. T., Reinecke, R., Schumacher, M., Shadkam, S., Telteu, C.-E., Trautmann, T., and Döll, P.: The global water resources and use model WaterGAP v2.2d: model description and evaluation, Geoscientific Model Development, 14, 1037–1079, https://doi.org/10.5194/gmd-14-1037-2021, 2021.

Müller Schmied, H., Cáceres, D., Eisner, S., Flörke, M., Herbert, C., Niemann, C., Peiris, T. A., Popat, E., Portmann, F. T., Reinecke, R., Shadkam, S., Trautmann, T., and Döll, P.: The global water resources and use model WaterGAP v2.2d - Standard model output, https://doi.org/10.1594/PANGAEA.918447, 2020.

Otosaka, I. N.: Improving estimates of ice sheet elevation change derived from AltiKa and CryoSat-2 satellite radar altimetry, Ph.D. thesis, University of Leeds, School Earth and Environment, 2021.

Peltier, W.: GLOBAL GLACIAL ISOSTASY AND THE SURFACE OF THE ICE-AGE EARTH: The ICE-5G (VM2) Model and GRACE, Annual Review of Earth and Planetary Sciences, 32, 111–149, https://doi.org/10.1146/annurev.earth.32.082503.144359, 2004.

Peltier, W. R., Argus, D. F., and Drummond, R.: Comment on "An Assessment of the ICE-6G_C (VM5a) Glacial Isostatic Adjustment Model" by Purcell et al., Journal of Geophysical Research: Solid Earth, 123, 2019–2028, https://doi.org/10.1002/2016jb013844, 2018.

Pfeffer, J., Cazenave, A., and Barnoud, A.: Analysis of the interannual variability in satellite gravity solutions: detection of climate modes fingerprints in water mass displacements across continents and oceans, Climate Dynamics, 58, 1065–1084, https://doi.org/10.1007/s00382-021-05953-z, 2022.

Roemmich, D. and Gilson, J.: The 2004–2008 mean and annual cycle of temperature, salinity, and steric height in the global ocean from the Argo Program, Progress in Oceanography, 82, 81–100, https://doi.org/10.1016/j.pocean.2009.03.004, 2009.

Save, H.: CSR GRACE and GRACE-FO RL06 Mascon Solutions v02, https://doi.org/10.15781/cgq9-nh24, 2020.

https://doi.org/10.5194/egusphere-2022-716
Preprint. Discussion started: 8 August 2022

Save, H., Bettadpur, S., and Tapley, B. D.: High-resolution CSR GRACE RL05 mascons, Journal of Geophysical Research: Solid Earth, 121, 7547–7569, https://doi.org/10.1002/2016jb013007, 2016.

Schröder, M., Lockhoff, M., Forsythe, J. M., Cronk, H. Q., Haar, T. H. V., and Bennartz, R.: The GEWEX Water Vapor Assessment: Results from Intercomparison, Trend, and Homogeneity Analysis of Total Column Water Vapor, Journal of Applied Meteorology and Climatology, 55, 1633–1649, https://doi.org/10.1175/jamc-d-15-0304.1, 2016.

Shepherd, A., Ivins, E. R., A, G., Barletta, V. R., Bentley, M. J., Bettadpur, S., Briggs, K. H., Bromwich, D. H., Forsberg, R., Galin, N., Horwath, M., Jacobs, S., Joughin, I., King, M. A., Lenaerts, J. T. M., Li, J., Ligtenberg, S. R. M., Luckman, A., Luthcke, S. B., McMillan, M., Meister, R., Milne, G., Mouginot, J., Muir, A., Nicolas, J. P., Paden, J., Payne, A. J., Pritchard, H., Rignot, E., Rott, H., Sorensen, L. S., Scambos, T. A., Scheuchl, B., Schrama, E. J. O., Smith, B., Sundal, A. V., van Angelen, J. H., van de Berg, W. J., van den Broeke, M. R., Vaughan, D. G., Velicogna, I., Wahr, J., Whitehouse, P. L., Wingham, D. J., Yi, D., Young, D., and Zwally, H. J.: A Reconciled Estimate of Ice-Sheet Mass Balance, Science, 338, 1183–1189, https://doi.org/10.1126/science.1228102, 2012.

Shepherd, A., Ivins, E., Rignot, E., Smith, B., van den Broeke, M., Velicogna, I., Whitehouse, P., Briggs, K., Joughin, I., Krinner, G., Nowicki, S., Payne, A., Scambos, T., Schlegel, N., A, G., Agosta, C., Ahlstrøm, A., Babonis, G., Barletta, V., Bjørk, A., Blazquez, A., Bonin, J., Colgan, W., Csatho, B., Cullather, R., Engdahl, M., Felikson, D., Fettweis, X., Forsberg, R., Gallee, H., Gardner, A., Gilbert, L., Gourmelen, N., Groh, A., Gunter, B., Hanna, E., Harig, C., Helm, V., Hogg, A., Horvath, A., Horwath, M., Khan, S., Kjeldsen, K., Konrad, H., Langen, P., Lecavalier, B., Loomis, B., Luthcke, S., McMillan, M., Melini, D., Mernild, S., Mohajerani, Y., Moore, P., Mottram, R., Mouginot, J., Moyano, G., Muir, A., Nagler, T., Nield, G., Nilsson, J., Noël, B., Otosaka, I., Pattle, M., Peltier, W., Pie, N., Rietbroek, R., Rott, H., Sørensen, L. S., Sasgen, I., Save, H., Scheuchl, B., Schrama, E., Schröder, L., Seo, K.-W., Simonsen, S., Slater, T., Spada, G., Sutterley, T., Talpe, M., Tarasov, L., van de Berg, W. J., van der Wal, W., van Wessem, M., Vishwakarma, B. D., Wagner, T., Wiese, D., Wilton, D., Wouters, B., and Wuite, J.: Antarctic and Greenland Ice Sheet mass balance 1992-2020 for IPCC AR6 (Version 1.0) [Data set], https://doi.org/10.5285/77B64C55-7166-4A06-9DEF-2E400398E452, 2021.

Simonsen, S. B., Barletta, V. R., Colgan, W. T., and Sørensen, L. S.: Greenland Ice Sheet Mass Balance (1992–2020) From Calibrated Radar Altimetry, Geophysical Research Letters, 48, https://doi.org/10.1029/2020gl091216, 2021.

Sun, Y., Riva, R., and Ditmar, P.: Optimizing estimates of annual variations and trends in geocenter motion and J2 from a combination of GRACE data and geophysical models, Journal of Geophysical Research: Solid Earth, 121, 8352–8370, https://doi.org/10.1002/2016jb013073, 2016.

Swenson, S., Chambers, D., and Wahr, J.: Estimating geocenter variations from a combination of GRACE and ocean model output, Journal of Geophysical Research: Solid Earth, 113, https://doi.org/10.1029/2007jb005338, 2008.

Tapley, B. D., Watkins, M. M., Flechtner, F., Reigber, C., Bettadpur, S., Rodell, M., Sasgen, I., Famiglietti, J. S., Landerer, F. W., Chambers, D. P., Reager, J. T., Gardner, A. S., Save, H., Ivins, E. R., Swenson, S. C., Boening, C., Dahle, C., Wiese, D. N., Dobslaw, H., Tamisiea, M. E., and Velicogna, I.: Contributions of GRACE to understanding climate change, Nature Climate Change, 9, 358–369, https://doi.org/10.1038/s41558-019-0456-2, 2019.

Velicogna, I., Mohajerani, Y., A, G., Landerer, F., Mouginot, J., Noel, B., Rignot, E., Sutterley, T., Broeke, M., Wessem, M., and Wiese, D.: Continuity of Ice Sheet Mass Loss in Greenland and Antarctica From the GRACE and GRACE Follow-On Missions, Geophysical Research Letters, 47, https://doi.org/10.1029/2020gl087291, 2020.

Vishwakarma, B. D., Bates, P., Sneeuw, N., Westaway, R. M., and Bamber, J. L.: Re-assessing global water storage trends from GRACE time series, Environmental Research Letters, 16, 034 005, https://doi.org/10.1088/1748-9326/abd4a9, 2021.

https://doi.org/10.5194/egusphere-2022-716
Preprint. Discussion started: 8 August 2022

Watkins, M. M., Wiese, D. N., Yuan, D.-N., Boening, C., and Landerer, F. W.: Improved methods for observing Earth's time variable mass distribution with GRACE using spherical cap mascons, Journal of Geophysical Research: Solid Earth, 120, 2648–2671, https://doi.org/10.1002/2014jb011547, 2015.